Model Systems of Precursor Cellular Membranes: Long-Chain Alcohols Stabilize Spontaneously Formed Oleic Acid Vesicles

Adela Rendón,[†] David Gil Carton,[‡] Jesús Sot,[†] Marcos García-Pacios,[†] Ruth Montes,[†] Mikel Valle,[‡] José-Luis R. Arrondo,[†] Felix M. Goñi,[†*] and Kepa Ruiz-Mirazo[†§*]

[†]Unidad de Biofísica (CSIC-UPV/EHU), and Departamento de Bioquímica, Universidad del País Vasco, Bilbao, Spain; [‡]Unidad de Biología Estructural, CIC-Biogune, Parque Tecnológico, Derio, Bizkaia, Spain; and [§]Departamento de Lógica y Filosofía de la Ciencia, Universidad del País Vasco, Donostia-San Sebastián, Spain

ABSTRACT Oleic acid vesicles have been used as model systems to study the properties of membranes that could be the evolutionary precursors of more complex, stable, and impermeable phospholipid biomembranes. Pure fatty acid vesicles in general show high sensitivity to ionic strength and pH variation, but there is growing evidence that this lack of stability can be counterbalanced through mixtures with other amphiphilic or surfactant compounds. Here, we present a systematic experimental analysis of the oleic acid system and explore the spontaneous formation of vesicles under different conditions, as well as the effects that alcohols and alkanes may have in the process. Our results support the hypothesis that alcohols (in particular 10- to 14-C-atom alcohols) contribute to the stability of oleic acid vesicles under a wider range of experimental conditions. Moreover, studies of mixed oleic-acid-alkane and oleic-acid-alcohol systems using infrared spectroscopy and Langmuir trough measurements indicate that precisely those alcohols that increased vesicle stability also decreased the mobility of oleic acid polar headgroups, as well as the area/molecule of lipid.

INTRODUCTION

Biomembranes consist of a wide variety of both lipidic and peptidic components whose synthesis is metabolically controlled and highly regulated, according to the specific requirements of each living cell at a particular moment or stage in its development, which accounts for their complex dynamic behavior and their key role in the organization of any biological organism. However, it is not easy to understand how those sophisticated supramolecular structures could emerge from simpler membranes, or what these simpler membranes should look like. Recent investigations in the fields of origins of life and synthetic-protocell biology (1) have focused on fatty acid vesicles as one of the most plausible starting points in the evolution of biologically relevant lipid compartments (2–4). The work here reported takes the oleic acid system as an experimentally suitable model to study the general properties of this kind of simplified membrane compartment and analyzes in particular how the presence of alkanes and alcohols may influence some of the main biophysical features of the compartments.

Fatty acids, either unsaturated (e.g., oleic, myristoleic, or linoleic acid) or short-chained, saturated (e.g., octanoic or decanoic acid) can form vesicles in aqueous solution under diverse experimental conditions (5–14). These supramolecular aggregates, in comparison with standard liposomes, have quite remarkable properties: they are more permeable and dynamic structures (whose growth and reproduction can be achieved under laboratory conditions (15–19)), but they are also less stable than phospholipid vesicles, since their formation depends on a relatively narrow set of values of experimental parameters, e.g., pH and ionic strength.

According to Morigaki and Walde (20), fatty acid vesicles are characterized by two main features: 1), a critical aggregation concentration (CAC) several orders of magnitude larger than that of the usual phospholipids, as a result giving much more abundant and faster exchange processes between monomers in solution and the actual molecules of the bilayer aggregate (as well as more frequent flip-flop processes within the bilayer); and 2), the negative net charge of the aggregate as a whole, since these vesicles typically form through the conjunction of a fatty acid (in a neutral, nonionized state) and its respective soap (negatively charged) or conjugated salt (if the counterion is included). More specifically, what determines whether closed bilayers form or not is the ratio between those two amphiphilic components, the neutral fatty acid and the soap, so the degree of protonation of the terminal carbonyl group (and, therefore, the pH of the solution) becomes a critical variable in the system. Thus, although vesicle formation in principle would not be favored by the molecular properties of single-chain lipids with a conical geometry (i.e., spontaneous tendency to form micelles), the creation of molecular pairs through hydrogen bonds between neutral fatty acid and anionic soap/salt (21), which would then adopt a more cylindrical geometry, makes possible their spontaneous assembly into bilayered closed structures.

As a result, if the pH of the system is maintained near the pKa of the fatty acid, favoring the balance between its deprotonated and protonated states (i.e., the stable union of pairs) and, in addition, the monomer concentration is above the minimum concentration threshold for molecular aggregation (CAC), then the formation of self-assembled

Submitted July 21, 2011, and accepted for publication December 9, 2011.

*Correspondence: felix.goni@ehu.es or kepa.ruiz-mirazo@ehu.es

Editor: Heiko Heerklotz.

0006-3495/12/01/0278/9 $2.00

doi: 10.1016/j.bpj.2011.12.026

vesicular structures is observed. If pH varies and moves away from the pKa value, the system will tend to other states of aggregation: micelles (typically, in the alkaline region) or other, less regular supramolecular structures, like droplets (typically at lower pH).

However, the pH range in which the vesicular phase is stable can be extended in mixed systems, as Apel and colleagues (22) have demonstrated, using short-chain fatty acids and alcohols. The presence of an alcohol whose chain length is similar to that of the fatty acid (but with a pH-insensitive headgroup) is supposed to be an alternative neutral component of the pair when the proportion of uncharged fatty acid is low. This happens when pH is increased significantly above the pKa, provoking excess of fatty acid in deprotonated states. Moreover, since pure fatty acid vesicles are not very realistic membrane models, working with mixtures is becoming a research target itself (13,23–25), and this is actually a good strategy to overcome some of the problems faced with the pure systems (26).

In that context, the primary target of this article is to investigate the spontaneous formation of aggregates of a particular fatty acid (oleic acid) in aqueous solution, characterizing the different aggregation phases as a function of pH and other experimental variables, like osmolarity, studying their entrapment capacity and analyzing in particular the influence that the presence of alcohols and alkanes of diverse chain lengths may have on the system. A long-chain (C18) fatty acid has been used to mimic more closely the thickness of present-day membranes, even if this required the inclusion of a double bond to make the molecule amenable to vesicle formation at room temperature. Our studies are complementary to a recently published report on micelle-vesicle equilibrium in the oleic/oleate system (27).

We therefore aim to gain further knowledge on how simple amphiphilic molecules (certainly simpler than the glycerophospholipids found in cell membranes) self-assemble into closed bilayers, and on the stability and permeability properties of the latter. As mentioned above, this type of vesicle could be a good model to study protocellular systems (6,7,28,29), namely possible precursors of present-day cellular membranes, without disregarding other potential applications they may have in the biotechnological domain.

MATERIALS AND METHODS

Materials

Oleic acid (C18:1) was from Merck (Darmstadt, Germany), and the various salts were obtained by titration of the oleic acid with the corresponding hydroxides. Methanol and chloroform were from Fisher (Suwanee, GA). All other chemicals were purchased from Sigma-Aldrich (St. Louis, MO).

Preparation of vesicles

Oleic acid vesicles were prepared by injecting an aqueous suspension of 3.15 M oleic acid (OA) into 0.2 M sodium bicine buffer at different pH values, typically 8.5. In experiments involving titration, the samples were initially brought to higher pH by addition of NaOH (micellar phase), and later adjusted by addition of HCl to the final pH values required. Final OA concentrations were in the range 1–20 mM.

Mixed vesicles tested included OA with hexanol, octane, octanol, decanol, dodecane, dodecanol, tetradecanol, hexadecane, hexadecanol, octadecane, and octadecanol (20:1,10:1, 5:1, and 2:1 molar ratios, 5 mM total concentration of fatty acid). Mixed-vesicle preparations were achieved by dissolving initially both fatty acid and alkane or alcohol in chloroform, which was then evaporated under nitrogen flow. Later, the mixture was resuspended at 21°C in 0.2 mM bicine, pH 8.5, and incubated at room temperature for 16 h before assay.

Buffer preparation

We prepared 0.2 M bicine by dissolving bicine in ultrapure water and adjusting the pH by addition of small amounts of 1 M HCl or 1 M NaOH to pH 8.5 (unless otherwise specified).

Turbidity measurements

Turbidity was measured with a Cary 300 Bio UV/vis multicell spectrophotometer from Varian (Sydney, New South Wales, Australia), using quartz cells with a path length of 1.0 cm, at $\lambda = 400$ nm.

Dynamic light scattering

Dynamic light scattering (DLS) measurements of particle sizes were carried on a Malvern Zetasizer nano System. This instrument was equipped with a 4 mW He-Ne LASER of 633 nm wavelength, and an Avalanche photodiode detector (quantum efficiency >50% at 633 nm) located at 173° from the incident beam direction in a backscatter position. The temperature of the sample holder was stabilized at 25°C through a Peltier thermostat. Samples were introduced into plastic 50–2000-μl capacity disposable cuvettes (UVette, Eppendorf, Hamburg, Germany).

Release/entrapment through fluorescence measurements

Vesicle leakage was estimated as an increase in absorbance at 500 nm, measured in a spectrofluorometer FluoroMax-3 (Horiba, Kyoto, Japan). Release of aqueous contents was assessed using the ANTS/DPX fluorescent probe system (described in Ellens et al. (30)). For measurements of vesicle leakage, lipids were hydrated in bicine 0.2 M, pH 8.5. Nonentrapped ANTS/DPX was removed by gel filtration on Sephadex G-25 columns. Fluorescence measurements were carried out in an LS-50B PerkinElmer (Waltham, MA) spectrofluorometer, at room temperature (21 ± 1°C) and with continuous stirring. The osmolality of intra- and extravesicular solutions was measured in a cryoscopic osmometer (Osmomat 030, Gonotec, Berlin, Germany) and adjusted to 0.3 Osm/kg by adding NaCl. Fluorescence scales were calibrated as described previously (31). With pure buffer in the cuvettes, 0% release was measured; 100% release was induced by addition of the nonionic detergent Triton X-100, known to permeabilize model and cell membranes, to a final 1 mM concentration. Excitation light was adjusted to 490 nm. An interference filter (520 nm) was used to avoid scattered excitation light.

Cryo-electron microscopy

Cryo-electron microscopy (cryo-TEM) is a suitable technique for direct visualization of surfactant aggregates ranging in size from 5–10 nm to 1 μm, at the same time minimizing artifacts due to sample preparation/ fixation (through staining). The sample was placed in the controlled environment of the vitrification chamber at room temperature, where the relative

humidity was kept close to saturation to prevent water evaporation from the sample. A 5-μl drop of the aqueous solution was placed on carbon-coated holey film supported by a TEM copper grid. Most of the liquid was removed by careful blotting with absorbent filter paper to create a thin liquid film. The sample was then rapidly plunged into liquid ethane and cooled by liquid nitrogen to its melting temperature to obtain a vitrified film. The vitrified specimen was stored under liquid nitrogen and then transferred into the electron microscope (Jeol JEM-2200FS) operating at 200 kV with an underfocus of 3–5 μm. The working temperature was kept below -175°C, and the images were collected under low-dose conditions with a CCD camera (UltraScan 4000, Gatan, Pleasanton, CA).

Preparation of giant unilamellar vesicles and fluorescence microscopy

Giant unilamellar vesicles (GUVs) were prepared by injecting an aqueous solution of 3.15 M OA into sodium bicine buffer (0.2 M, pH 8.5). OA (3.15 M in chloroform) was evaporated under nitrogen flow, and the lipid was resuspended at 25°C in 0.2 mM bicine at pH 7.5, 8.5 or 10. The hydrated sample was homogenized, passing it five times through a 25-mm, 23-gauge needle. A small aliquot (~3 μl) of aqueous solution was deposited onto the platinum electrodes and allowed to dry in a vacuum chamber for 30 min. Giant vesicles were obtained by using the electroformation method developed by Angelova et al. (32): a low-frequency AC field (sinusoidal wave function with a frequency of 10 Hz and an amplitude of 2.5 V) was applied for 120 min at 75°C in the same, preheated, buffer. Thin-layer chromatography revealed no lipid degradation under these conditions. The vesicles were directly observed with an inverted confocal microscope (TE2000 U, Nikon, Melville, NY). The excitation wavelength for DiIC18 (bilayer concentration 0.4 mol %) was 488, and the fluorescence signal was collected using a bandpass filter of 593 $\pm$ 40 nm. The objective used was a 40$\times$ oil immersion, NA 1.0 objective.

Infrared spectroscopy

For this set of measurements, OA (5 mM) was suspended in chloroform and mixed with the corresponding alcohol/alkane (also in chloroform), whenever required, at either a 2:1 or a 10:1 mol ratio. We vacuum-dried 40 μL of each sample overnight on a 56-mm-diameter CaF_2 window (IR Select, Spectroscopy Central, Warrington, UK). Before measuring, the films were resuspended in 40 μL D_2O (Merck), covered with another CaF_2 window interposing a 56-μm pathlength teflon spacer (Harrick Scientific, Ossining, NY) and mounted on a Harrick cell. We acquired 360 scans and took the average for each spectrum using an MCT detector in a Nexus 870 infrared (IR) spectrometer (Thermo Nicolet, Madison, WI).

Monolayer surface pressure measurements

In this case, samples were similarly prepared in chloroform and then mixed with the alcohol/alkane at a 10:1 mol ratio. Monolayers were then spread from 22 μl of chloroform solution onto a 235-cm^2 Teflon trough filled with 110 ml 10 mM Tris and 150 mM KCl, pH 8.5, at 22°C. The film was relaxed for 30 min at 0 mN/m and later compressed to the collapse phase at a speed of 0.15 $nm^2\ mol^{-1}\ min^{-1}$. Surface pressure and film area were measured in a Micro-Processor Interface IU4 (NIMA, Coventry, UK). The reproducibility of experiments was within the maximum standard error of ± 1 $Å^2$ for molecular areas.

RESULTS

The OA-water system

To analyze the different aggregation phases of OA in aqueous solution (originally determined by others (5,8,9)) with our experimental setting and to study the conditions under which vesicles form spontaneously, we first used turbidimetry (absorbance at 400 nm) and observed three clearly differentiated regions as the pH of the solution was modified. As expected from previous work with this and other fatty acids, the slope of the absorbance profile undergoes two clear changes, marking the transition from micelles to vesicles (around pH 9 in this case) and from vesicles to droplets (just below pH 8). This is shown in Fig. 1, *A* and *B* (for different OA concentrations): the micellar phase (high pH) is characterized by an almost flat slope, whereas in the vesicular phase (pH around pKa 8.5 for OA), the slope becomes moderate, and in the droplet phase (neutral pH or below), absorbance values increase markedly (steeper subset of points). These experiments rely on the fact that the formation and breakdown of fatty acid supramolecular aggregates, after pH variations, are relatively fast processes.

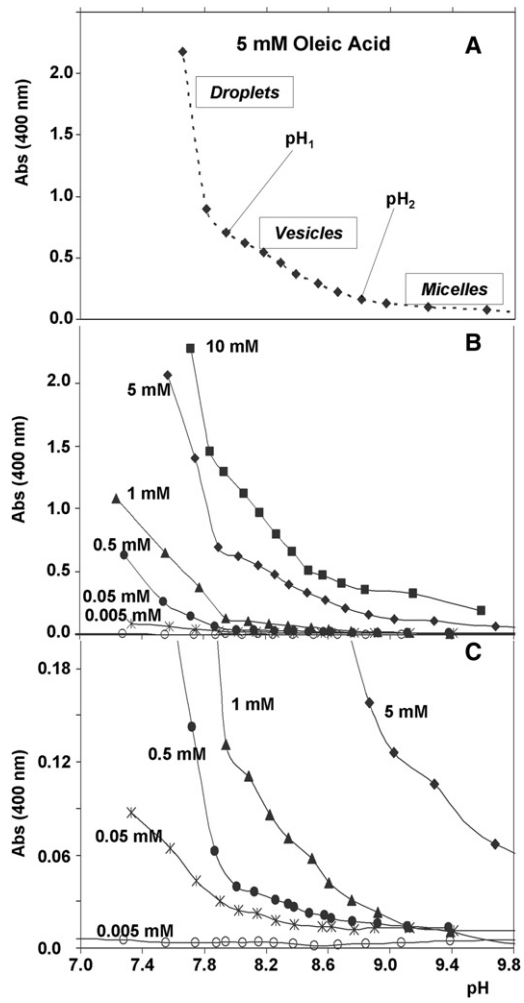

FIGURE 1 Absorbance profiles as a function of pH for the pure OA system. (*A*) [OA] = 5 mM was chosen as the control condition. The pH values that mark the two main phase transitions (pH_1 and pH_2) are indicated. (*B*) Profiles for various concentrations of OA. (*C*) Close-up to show more clearly the CAC threshold.

For the case of vesicle formation, the longest expected times are in the range between 1 s and 1 min (33); for vesicle breakdown and micellar processes, they are much shorter.

Two additional remarks should be made here: first, the observation that titration curves change if the starting point of the system is changed (in our experiments, since the micellar state is molecularly more ordered or homogeneous than the droplets, we typically started from high pH values, to contribute to a smoother vesicle self-assembly). For instance, the turbidity of a sample directly prepared at pH 8.5 is typically higher than the turbidity of the same sample, after bringing it up to the micellar phase (high pH) and titrating it down, back to pH 8.5. This asymmetry or irreversibility in the oleic system is not surprising, given the intrinsic dependence of this type of supramolecular self-assembly process on initial conditions—and on the preparation procedure in general (34). Second, we confirmed the existence of a CAC below which no vesicles are formed (see Fig. 1 *C*). Through the analysis of these turbidity profiles for different OA concentrations, the 5 mM condition, well above the CAC, was selected for subsequent experiments.

With the aim of clarifying, as far as possible, the source of the aforementioned irreversibility, we carried out a series of experiments in which turbidity was measured under different conditions of pH and osmolarity, using independently prepared samples (i.e., fixed values of pH and ionic strength for each of them) and waiting for different time spans (24 and 48 h) after preparation. The results of these experiments are condensed in Fig. S1 in the Supporting Material, which essentially shows that although variations in osmolarity do not seem to have a large effect at pH around the pKa (± 0.3) of the fatty acid, moving away from the 8–8.5 pH region, changes in the overall osmolite concentration do have more radical consequences in the state of the system, as measured by variations in A_{400}. There is, anyhow, an overall limit in terms of the osmotic strength that the system can withstand: the reported data at osmolarity values >0.8 are no longer reliable, since samples become nonhomogenous, i.e., they are not opalescent any more but contain macroscopic aggregates, which precipitate in the absence of stirring. Furthermore, we confirmed that the most orderly and stable way to produce vesicles is when osmolarity values remain rather low (<0.4) and, optimally, when the system reaches the vesicle stability phase from the higher pH region (micellar phase).

DLS measurements consistently confirmed that the mean size of OA aggregates increases as the pH decreases (Fig. 2), and the average diameters obtained are compatible with the predicted phase changes (from micelles to vesicles to droplets) as pH is decreased. This is in agreement with recent observations by Dejanovic et al. (27). Morphology of the particles in suspension was examined by cryo-TEM. Vesicular shapes were found mainly at pH between 7.8 and 9. Above and below those limits vesicles coexist with other

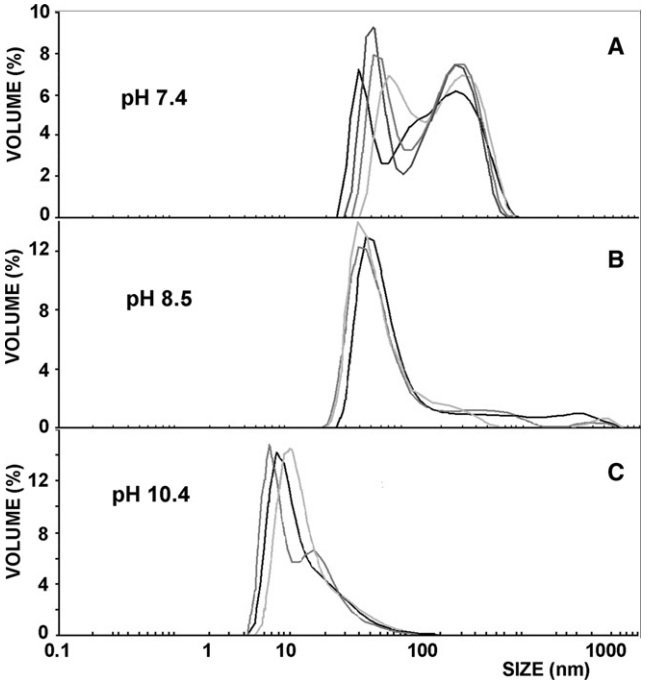

FIGURE 2 DLS size distributions of the population of aggregates at different pH values. As pH decreases there is a progressive increase in the mean size and heterogeneity (polydispersion index) of the population.

aggregation states of OA, like micelles or droplets, suggesting that pure phases may be separated from each other in the phase diagram by regions of phase coexistence. However, cryo-TEM images at different pH (see Fig. 3, *A–C*) demonstrate that vesicles constitute the statistically relevant (or spontaneously favored) aggregation state at pH ~ pKa, even if the size and lamellarity of the population is very heterogeneous, as one would expect in nonextruded suspensions.

We collected an additional piece of evidence by means of entrapment/release studies to verify that most of the aggregates formed under these conditions (pH ~ pKa) were stable vesicles, as compared to those found in other pH regions. According to the fluorimetric results shown in Table 1, obtained through the encapsulation and progressive release of the ANTS/DPX quenching pair, at different pH values, it is clear that only when pH is ~8.5 do OA aggregates show a significant capacity for solute entrapment.

Finally, we also checked that OA molecules can form GUVs (Fig. 3 *D*). However, in these cases, one cannot claim that there is a spontaneous self-assembly process: rather, vesicle formation is induced by an electric (low-frequency) AC field applied on a platinum electrode in continuous contact with the aqueous solution. Vesicle growth is, therefore, electrodynamically directed by the progressive and ordered accumulation of (both charged and uncharged) OA molecules on the electrode. Under these conditions, the formation of giant vesicles was achieved, even at pH values relatively removed from the pKa, although in those

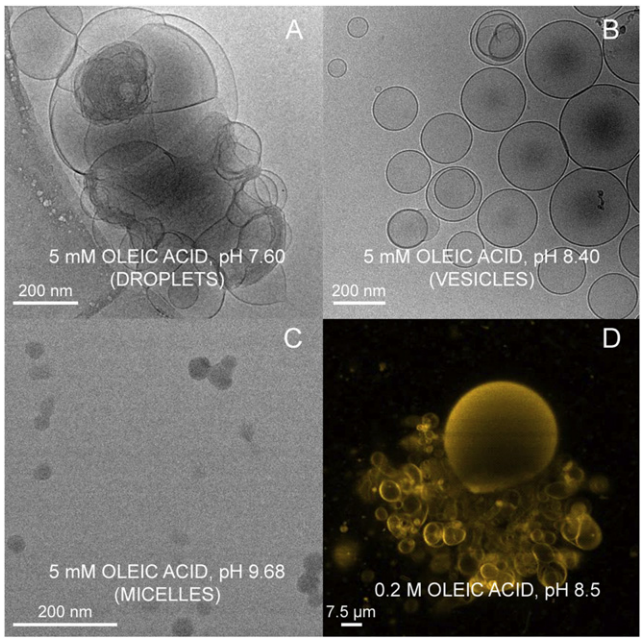

FIGURE 3 Cryo-TEM and confocal microscopy images of the OA system (5 mM) in bicine buffer (0.2 M) at different pH values. (*A–C*) Cryo-TEM images at pH 7.6 (large aggregates—droplets) (*A*), pH 8.4 (vesicles) (*B*), and pH 9.7 (micelles) (*C*). (*D*) Confocal image (note the different scale) showing a giant vesicle of OA (pH 8.5) with a background of smaller ones, in the formation process.

cases the mean sizes in the population of GUVs obtained were typically smaller.

Mixtures and induced stability changes

We further investigated the influence that alcohols and alkanes could have on the stability of OA vesicles. Previous experimental studies with shorter, saturated fatty acids (22) indicated that the presence of alcohols could enhance the pH range in which this type of vesicle is spontaneously formed and reduce the value of the CAC. Therefore, we tried combining alcohols and alkanes of different chain lengths with OA in diverse ratios before hydrating them in the bicine buffer (i.e., before the supramolecular aggregates were actually formed). Note that alkanes are not soluble, nor can they be dispersed in buffer unless in mixtures with OA (35).

TABLE 1 Percent aqueous content entrapped in OA aggregates

	Entrapment (%)		
Time (min)	pH 7.5	pH 8.5	pH 10
0	5 ± 0.73	75 ± 0.95	14 ± 0.97
60	1 ± 1.82	56 ± 1.34	13 ± 0.24
180	<1	43 ± 1.57	12 ± 0.60

Content release was measured at various times after removal of nonentrapped solutes by column chromatography (see Methods). 100% release was measured after addition of 1 mM Triton X-100. Values are expressed as the mean ± SD (n = 3).

Starting generally from alkaline conditions (pH ~10), we titrated these mixed systems toward progressively lower pH values, following the evolution of their A_{400}. The results obtained in this way are summarized in Fig. 4, *A–F*, whose most striking conclusion regards the difference in the effect of alcohols and alkanes. In fact, alkanes (Fig. 4, *A* and *D*) have hardly any effect on the oleic system, except for some blurring of the slope changes in the curve that could be interpreted as a softening of the phase transitions, whereas alcohols clearly raise the A_{400} of the samples, even at relatively high pH values. At these pH values, A_{400} measurements remain very low in the pure-control-system, since micelles constitute the spontaneous aggregation state under those conditions, and their contribution to turbidity is negligible. Thus, the presence of alcohols seems to favor the formation of bigger aggregates, mainly vesicles, as can be observed in Fig. 5, provided that the length of their chain is within a certain range. Note that, particularly for the shorter-chain alcohols, partition may be taking place between the aqueous and lipidic environments. For an original alcohol/OA (1:10) ratio, the use of different-chain-length alcohols leads to significant increases in turbidity for alcohols with chains in the 10- to 14-carbon range (Fig. 4, *B* and *E*). For a given alcohol chain length in the mixture with OA, the effect on turbidity was dose-dependent (Fig. 4, *C* and *F*). These results correlated well with the cryo-TEM images, where the largest aggregates appeared in those samples for which turbidity was highest (Fig. 5, *A–D*). If the alcohol was either too short or too long, no vesicles were detected, confirming some structural compatibility requirement.

Additional experiments were carried out to study the effect that this type of mixture could have in terms of the general capacity for entrapment and the rate of content release of the vesicles. As in the control experiments with pure OA vesicles, the ANTS/DPX assay was used. We found that no matter the lipid composition, the release was never complete unless Triton was eventually added to the sample: the fluorimetric profile reached a plateau in all cases (see Fig. 6). As reported in Fig. 7, *A* and *B*, we analyzed the initial stages of the process, calculating the slope of the release curves. In all cases, slope is significantly reduced when alkanes or alcohols are present (Fig. 7 *A*). In other words, the initial velocity of the release is generally decreased by the use of mixtures, regardless of whether an alcohol or an alkane is involved, and also regardless of the concentration ratio for the mixture (Fig. 7 *A*). Then, if we focus the attention on the final states of the samples, when an apparent equilibrium has been reached, their relative fluorescence values (in comparison with the 100% release values obtained after the addition of Triton), indicate that the proportion of remaining dye depends on the nature of the additive. Although it lowers the rate of dye release (Fig. 7 *A*), octanol allows a larger proportion of dye to leave the vesicles (Fig. 7 *B*). However, both hexadecane and

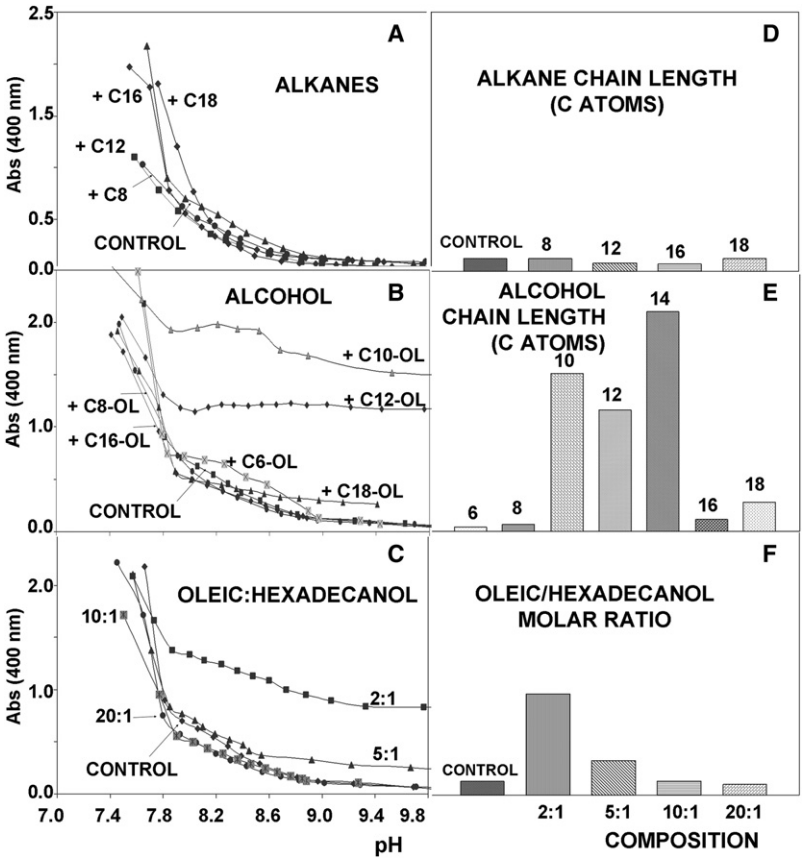

FIGURE 4 Absorbance profiles as a function of pH for different mixed systems (in all cases, concentration was fixed at [OA] = 5 mM). (*A*) Mixtures with alkanes of different chain length, at a fixed 1:10 (alkane/OA) ratio. No changes in this general behavior were observed with higher relative amounts of alkane, up to 1:2 ratios. (*B*) Mixtures with alcohols of different chain length, at a fixed 1:10 (alcohol/OA) ratio. (*C*) Mixtures with hexadecanol, at different ratios: the higher the relative amount of alcohol, the stronger the effect on turbidity. Graphs on the right-hand side (*D–F*) represent the corresponding absorbance values for a fixed pH (9.2).

hexadecanol not only decrease the release rate (Fig. 7 *A*) but also allow a higher proportion of liquid contents to remain in the vesicles (Fig. 7 *B*).

On the mechanism of stabilization

With the aim of understanding the molecular mechanisms underlying the observed stabilization, mixtures of OA with alkanes or alcohols in aqueous media were examined by IR spectroscopy and in the Langmuir trough. As for the first technique, the 1600–1800 cm^{-1} regions of the resulting spectra, corresponding to the stretching vibration of the carbonyl groups of OA, are shown in Fig. 8. Other spectral regions did not provide significant new information. However, the data in Fig. 8 point to a motional stabilization of the OA polar headgroups in the presence of tetradecanol (Fig. 8 *C*), but not in the presence of hexadecanol (Fig. 8 *A*) or of the corresponding alkanes (Fig. 8, *B* and *D*). In all cases, the absorption maximum remains unaltered by the added alcohol, which does not support the idea that the long-chain alcohols would stabilize the system through an H-bond network. Instead, it is the width of the absorption band that is decreased by tetradecanol, i.e., by one of the optimum stabilizers at the 10:1 mol ratio (according to the results summarized in Fig. 4 *E*), but not by hexadecanol, which was not active in that previous set of experiments. The long-chain alkanes C14 and C16 show an opposite effect: they actually increase the width of the OA carbonyl stretching vibration (Fig. 8, *B* and *D*). The width of these spectral bands has been directly related to the librational motions of the corresponding groups (36).

These results were complemented and confirmed by studies of the surface behavior of OA in mixtures with long-chain alcohols or alkanes, at 10:1 mol ratio. The mixtures were spread on an air-water interface and compressed at a constant rate. Changes in surface pressure were recorded with a Langmuir trough until the lipid monolayer collapsed. The data in Fig. 9 *A*, expanded in Fig. 9 *B*, show that C10, C12, and C14—but not C16 or C18—alcohols compress the monolayer, i.e., reduce the surface area/molecule of lipid at a given imposed lateral pressure. This correlates very well with the mixtures giving rise to vesicles in an extended range of pH in Fig. 4 *E*. No chain-length-dependent effects were observed with the corresponding alkanes (π-area plots not shown). Thus, the Langmuir trough experiments demonstrate that the C10–C14 alcohols interact with OA, decreasing the average area occupied by each lipid molecule (chain). Since the IR results indicated a decreased motion of the OA polar headgroup, these alcohols may have a dual role in stabilizing OA aggregates, at both the hydrophobic-chain and polar-headgroup levels. Although our data do not provide specific information as

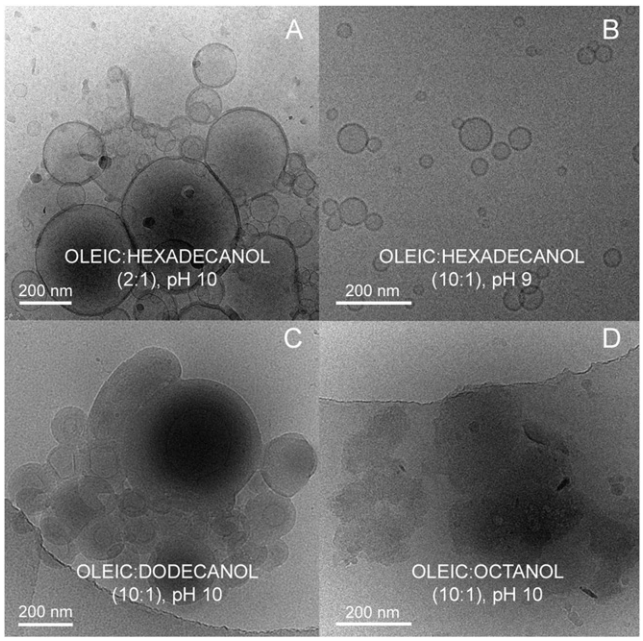

FIGURE 5 Cryo-TEM images of various OA-alcohol mixtures ([OA] = 5 mM) in bicine buffer (0.2 M) at high pH values. The images support the absorbance profiles results shown in Fig. 4, demonstrating that vesicles and aggregates of vesicles form in the strongly alkaline region (*A–C*) but not for a short-chain alcohol, octanol (*D*).

to the location of alkanes/alcohols within the OA bilayer, the IR spectra shown in Fig. 8 clearly reflect that in most—if not all—cases, the lipid-water interface is perturbed by both alcohols and alkanes, though perhaps in a different way.

DISCUSSION AND PERSPECTIVES

The experimental characterization of the OA system (Figs. 1–3) reveals several of its most salient features. First, the different aggregation states (micelles, vesicles, and droplets) depend on the pH of the solution. Second, osmolarity has a critical influence on the stability of the aggregates, particularly the vesicles, as reported by Monnard and colleagues (11) for decanoic acid vesicles. Third, the capacity for entrapment of these spontaneously formed vesicle systems was also verified.

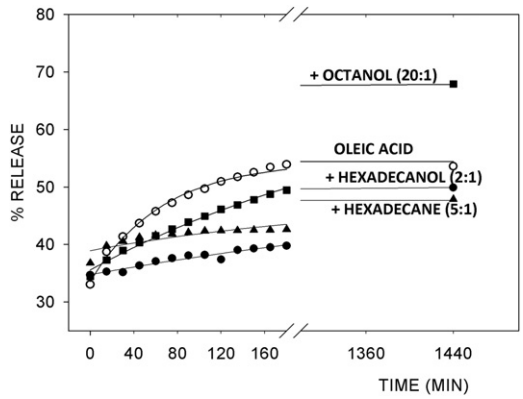

FIGURE 6 Release of entrapped water-soluble dyes. Release kinetics of the ANTS/DPX pair, whose fluorimetric signal was followed for ~24 h, after removal from the external milieu by a gel filtration column, showing OA control (*open circles*), OA/octanol (20:1) (*solid squares*), OA/hexadecane (5:1) (*solid triangles*), and OA/hexadecanol (2:1) (*solid circles*). After addition of Triton X-100, release measured 100%.

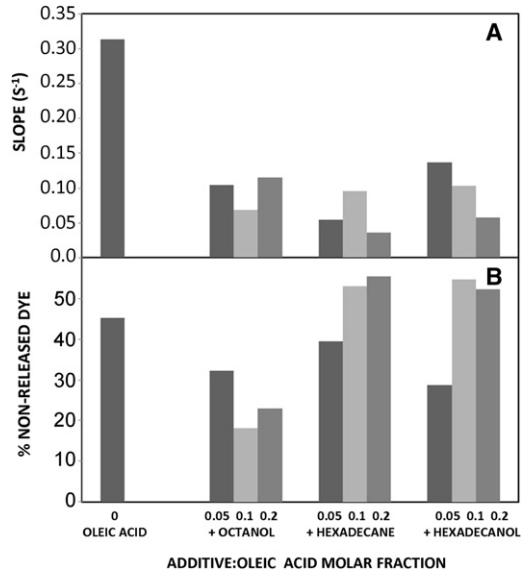

FIGURE 7 Effect of additives on the release of entrapped dyes. (*A*) Changes in the intial slopes (rates). (*B*) Percent of nonreleased dye (taking as the 100% reference the value obtained after Triton addition).

We have further demonstrated that mixtures with alcohols (but not with alkanes) have a strong effect on the aggregation properties of the OA system, making possible the spontaneous generation of vesicles for pH values well above the pKa of the acid. This confirmed similar experimental results obtained by Apel et al. (22) with shorter fatty acids. The relevance of this finding can be better appreciated in the context of the appearance in the biosphere of the first compartments and their subsequent development through increasingly complex molecules, from fatty acids to the phospholipids that build up the present membranes. Hargreaves and Deamer (7) had already observed that dispersion of dodecanoate gave rise to vesicles in a wider pH range when dodecanol was also present. Monnard and Deamer (37) suggest that if alcohols manage to come together with fatty acids at some initial stage, for instance, by providing additional stability to the vesicles, as supported also by our results, the production of glycerol lipid derivatives would be facilitated, as an intermediate step toward amphiphilic compounds whose polar head included a phosphate group. Several pieces of evidence (25,38) point in analogous directions and highlight the importance of studying the prebiotically available compounds (e.g., simple, single-stranded fatty acids) that only later, with the advent of biosynthetic, protometabolic pathways, would

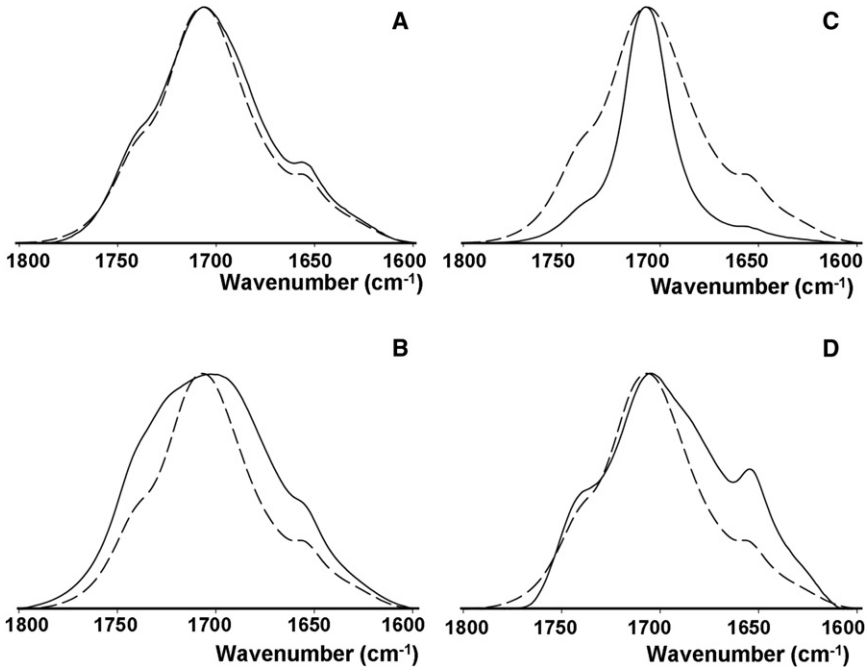

FIGURE 8 The baseline-corrected 1600–1800 cm^{-1} region of the IR spectra of OA, either pure or in mixtures with alkanes or alcohols. This spectral region corresponds to the stretching vibration of the fatty acid carbonyl group. (*A*) OA ± C16-alcohol (2:1). (*B*) OA ± C16-alkane (2:1). (*C*) OA ± C14-alcohol (10:1). (*D*) OA ± C14-alkane (10:1). The spectrum of pure OA is drawn with a dashed line.

develop into more complex (two-chain-stranded and larger polar head) lipids (39).

Our results therefore confirm those by Apel and colleagues (22) and extend them to long-chain fatty acids and alcohols. In this context, it is not realistic to assume, as a premise, the presence of pure vesicles made of a single type of compound, which is why we seek to combine OA with other simple compounds, like alcohols and alkanes of diverse chain lengths, which surely coexist with fatty acids in any prebiotic scenario. In addition to the analysis of vesicle stability discussed above, the content-release studies indicate other possible advantages of mixtures, namely, slower release profiles and a higher entrapment capacity of the vesicles. Moreover, the IR spectroscopic and Langmuir trough experiments carried out provide solid evidence that certain alcohols (C10, C12, and C14) compress laterally the OA aliphatic chains and reduce the motility of their carbonyl groups. These experiments thus help to build a coherent molecular explanation of the observed macroscopic changes in lipid aggregation and vesicle stability.

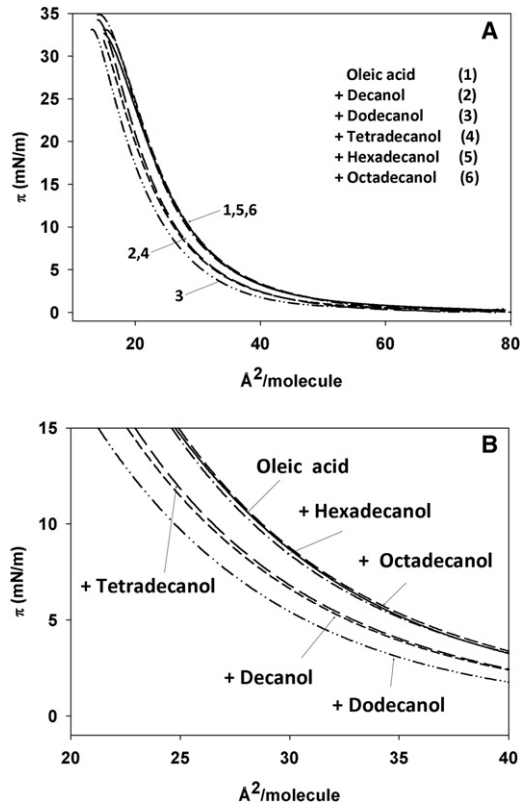

FIGURE 9 Compression isotherms of pure OA and of mixtures with alkanes or alcohols at a 10:1 mol ratio. Measurements were carried out at 22°C.

The approach followed here could be extended in various ways. Mixtures with other compounds, not just alcohols and alkanes, should be tried (13,23). With the appropriate combination of amphiphiles, many of the difficulties that this hypothetical scenario for the origin of cell membranes poses, like the apparent lack of stability of fatty acid vesicles, could be overcome. A growing number of laboratories are becoming aware of the relevance of using increasingly complex mixtures in the quest to elaborate more solid and realistic membrane models, not only in the context of the origins of cellularity, but also for a better understanding of biomembrane properties and behavior at large.

SUPPORTING MATERIAL

A figure is available at http://www.biophysj.org/biophysj/supplemental/S0006-3495(11)05455-5.

The authors are grateful to Dr. P. Walde (Eidgenössische Technische Hochschule, Zürich, Switzerland) for critically reading a previous version of the manuscript.

This work was supported in part by grants from the Spanish Ministerio de Ciencia e Innovación (MICINN) to K.R.M. (FFI2008-06348-C02-01) and F.M.G. (BFU2007-62062), and from the University of the Basque Country to F.M.G. (GIV06/42). K.R.M. holds a Ramón y Cajal Research Fellowship and also acknowledges support from COST Action CM0703.

REFERENCES

1. Solé, R. V., A. Munteanu, …, J. Macía. 2007. Synthetic protocell biology: from reproduction to computation. *Philos. Trans. R. Soc. Lond. B Biol. Sci.* 362:1727–1739.
2. Pohorille, A., and D. Deamer. 2009. Self-assembly and function of primitive cell membranes. *Res. Microbiol.* 160:449–456.
3. Mansy, S. S., and J. W. Szostak. 2009. Reconstructing the emergence of cellular life through the synthesis of model protocells. *Cold Spring Harb. Symp. Quant. Biol.* 74:47–54.
4. Chen, I. A., and P. Walde. 2010. From self-assembled vesicles to protocells. *Cold Spring Harb. Perspect. Biol.* 2:a002170.
5. Ekwald, P., and L. Mandell. 1969. Solutions of alkali soaps and water in fatty acids. I. Region of existence of the solutions. *Kolloid Z. Polym.* 233:938–944.
6. Gebicki, J. M., and M. Hicks. 1973. Ufasomes are stable particles surrounded by unsaturated fatty acid membranes. *Nature.* 243:232–234.
7. Hargreaves, W. R., and D. W. Deamer. 1978. Liposomes from ionic, single-chain amphiphiles. *Biochemistry.* 17:3759–3768.
8. Cistola, D. P., D. Atkinson, …, D. M. Small. 1986. Phase behavior and bilayer properties of fatty acids: hydrated 1:1 acid-soaps. *Biochemistry.* 25:2804–2812.
9. Cistola, D. P., J. A. Hamilton, …, D. M. Small. 1988. Ionization and phase behavior of fatty acids in water: application of the Gibbs phase rule. *Biochemistry.* 27:1881–1888.
10. Walde, P., R. Wick, …, P. L. Luisi. 1994. Autopoietic self-reproduction of fatty acid vesicles. *J. Am. Chem. Soc.* 116:11649–11654.
11. Monnard, P. A., C. L. Apel, …, D. W. Deamer. 2002. Influence of ionic inorganic solutes on self-assembly and polymerization processes related to early forms of life: implications for a prebiotic aqueous medium. *Astrobiology.* 2:139–152.
12. Chen, I. A., R. W. Roberts, and J. W. Szostak. 2004. The emergence of competition between model protocells. *Science.* 305:1474–1476.
13. Namani, T., and D. W. Deamer. 2008. Stability of model membranes in extreme environments. *Orig. Life Evol. Biosph.* 38:329–341.
14. Mansy, S. S. 2009. Model protocells from single-chain lipids. *Int. J. Mol. Sci.* 10:835–843.
15. Berclaz, N., M. Muller, …, P. L. Luisi. 2001. Growth and transformation of vesicles studied by ferritin labeling and cryotransmission electron microscopy. *J. Phys. Chem. B.* 105:1056–1064.
16. Hanczyc, M. M., S. M. Fujikawa, and J. W. Szostak. 2003. Experimental models of primitive cellular compartments: encapsulation, growth, and division. *Science.* 302:618–622.
17. Luisi, P. L., P. S. Rasi, and F. Mavelli. 2004. A possible route to prebiotic vesicle reproduction. *Artif. Life.* 10:297–308.
18. Chen, I. A., and J. W. Szostak. 2004. A kinetic study of the growth of fatty acid vesicles. *Biophys. J.* 87:988–998.
19. Stano, P., E. Wehrli, and P. L. Luisi. 2006. Insights into the self-reproduction of oleate vesicles. *J. Phys. Condens. Matter.* 18:S2231–S2238.
20. Morigaki, K., and P. Walde. 2007. Fatty acid vesicles. *Curr. Opin. Colloid Interface Sci.* 12:75–80.
21. Haines, T. H. 1983. Anionic lipid headgroups as a proton-conducting pathway along the surface of membranes: a hypothesis. *Proc. Natl. Acad. Sci. USA.* 80:160–164.
22. Apel, C. L., D. W. Deamer, and M. N. Mautner. 2002. Self-assembled vesicles of monocarboxylic acids and alcohols: conditions for stability and for the encapsulation of biopolymers. *Biochim. Biophys. Acta.* 1559:1–9.
23. Namani, T., and P. Walde. 2005. From decanoate micelles to decanoic acid/dodecylbenzenesulfonate vesicles. *Langmuir.* 21:6210–6219.
24. Mansy, S. S., J. P. Schrum, …, J. W. Szostak. 2008. Template-directed synthesis of a genetic polymer in a model protocell. *Nature.* 454: 122–125.
25. Maurer, S. E., D. W. Deamer, …, P. A. Monnard. 2009. Chemical evolution of amphiphiles: glycerol monoacyl derivatives stabilize plausible prebiotic membranes. *Astrobiology.* 9:979–987.
26. Thomas, J. A., and F. R. Rana. 2007. The influence of environmental conditions, lipid composition, and phase behavior on the origin of cell membranes. *Orig. Life Evol. Biosph.* 37:267–285.
27. Dejanović, B., V. Noethig-Laslo, …, P. Walde. 2011. On the surface properties of oleate micelles and oleic acid/oleate vesicles studied by spin labeling. *Chem. Phys. Lipids.* 164:83–88.
28. Deamer, D. W., and J. P. Dworkin. 2005. Chemistry and physics of primitive membranes. *Top. Curr. Chem.* 259:1–27.
29. Walde, P. 2006. Surfactant assemblies and their various possible roles for the origin(s) of life. *Orig. Life Evol. Biosph.* 36:109–150.
30. Ellens, H., J. Bentz, and F. C. Szoka. 1985. H^+- and Ca^{2+}-induced fusion and destabilization of liposomes. *Biochemistry.* 24:3099–3106.
31. Nieva, J. L., F. M. Goñi, and A. Alonso. 1989. Liposome fusion catalytically induced by phospholipase C. *Biochemistry.* 28:7364–7367.
32. Angelova, M. I., S. Soléau, …, P. Bothorel. 1992. Preparation of giant vesicles by external AC fields. Kinetics and application. *Prog. Colloid Polym. Sci.* 89:127–131.
33. Morigaki, K., P. Walde, …, B. H. Robinson. 2003. Thermodynamic and kinetic stability. Properties of micelles and vesicles formed by the decanoic acid/decanoate system. *Colloids Surf. A Physicochem. Eng. Asp.* 213:37–44.
34. Marques, E. F. 2000. Size and stability of catanionic vesicles: effects of formation path, sonication and aging. *Langmuir.* 16:4798–4807.
35. Urbina, P., A. Alonso, …, J. Sot. 2006. Alkanes are not innocuous vehicles for hydrophobic reagents in membrane studies. *Chem. Phys. Lipids.* 139:107–114.
36. Castresana, J., J. M. Valpuesta, …, F. M. Goñi. 1991. An infrared spectroscopic study of specifically deuterated fatty-acyl methyl groups in phosphatidylcholine liposomes. *Biochim. Biophys. Acta.* 1065:29–34.
37. Monnard, P.-A., and D. W. Deamer. 2002. Membrane self-assembly processes: steps toward the first cellular life. *Anat. Rec.* 268:196–207.
38. Apel, C. L., and D. W. Deamer. 2005. The formation of glycerol monodecanoate by a dehydration condensation reaction: increasing the chemical complexity of amphiphiles on the early Earth. *Orig. Life Evol. Biosph.* 35:323–332.
39. Peretó, J., P. López-García, and D. Moreira. 2004. Ancestral lipid biosynthesis and early membrane evolution. *Trends Biochem. Sci.* 29:469–477.